CDF/ANAL/EXOTIC/CDFR/10123
Draft 1.0
May 13, 2010

Search for Randall-Sundrum Gravitons in 5.4 fb^{-1} Run II Data at CDF

Ray Culbertson and Tingjun Yang

FNAL

Abstract

This note describe a search for Randall-Sundrum model gravitons performed in the diphoton channel using 5.4 fb^{-1} Run II data collected in the CDF detector. 95% confidence limits on the production cross-section times branching ratio for Randall-Sundrum model gravitons decaying to diphotons are obtained, from which lower limits on the graviton mass for various width parameters are derived.

Contents

1 Introduction

The large hierarchy between the electroweak and apparent gravity scales is a primary mystery of particle physics. It is possible that the observed 4-dimensional (4D) value of the Planck scale, M_{Pl}, is not truly fundamental. In 1998 Arkani-Hamed, Dimopoulos and Dvali (ADD) [1] proposed the existence of n additional compact dimensions of volume V_n and relates the fundamental (4+n)D Planck scale, M, to M_{Pl} via $M_{Pl}^2 = V_n M^{2+n}$. Setting $M \sim$ TeV to remove the above hierarchy necessitates large extra dimensions compactified at the scale $\mu_c = 1/r_c = V_n^{-1/n} \sim$ eV-MeV depending on the number of extra dimensions n. This introduces another hierarchy between μ_c and the electroweak scale M.

In 1999 Randall and Sundrum (RS) [2] proposed an alternative scenario, where the hierarchy is generated by an exponential function of the compactification radius, called a warp factor, in a 5D nonfactorizable geometry, based on a slice of AdS_5 spacetime. In this scenario, a fundamental 5D mass scale m_0 will appear to have the physical mass in a 4D theory

$$m = e^{-kr_c\pi} m_0, \tag{1}$$

where $k \sim M_{Pl}$ is the AdS_5 curvature and r_c is the compactification radius. TeV scales are thus generated from fundamental scales of order M_{Pl} via a geometrical exponential warp factor. The hierarchy is reproduced if $kr_c \simeq 12$ and no additional hierarchies are generated. The compactification scale $\mu_c = 1/r_c$ is of the order of the Planck scale. Because of the small compactification radius, there are no deviations from Newton's law at experimentally accessible distances. Kaluza-Klein (KK) towers of gravitons result from compactification of the extra dimension, with masses given by [3]

$$m_n = kx_n e^{-kr_c\pi}, \tag{2}$$

where x_n is the n^{th} root of the Bessel function J_1. These masses are of order of a TeV, and KK gravitons can be detected as massive resonances in collider experiments. Two parameters control the properties of the RS model: the mass of the first KK graviton excitation $m_G = m_1$, and the constant $c = k/\overline{M}_{Pl}$, determining the graviton couplings and widths, where $\overline{M}_{Pl} = M_{Pl}/\sqrt{8\pi} = 2.4 \times 10^{18}$ GeV is the effective four-dimensional reduced Planck scale. The values of k must be large enough to be consistent with the apparent weakness of gravity, but small enough to prevent the theory from becoming nonperturbative [3]. Given these considerations, we examine values in the

range $0.01 < k/\overline{M}_{Pl} < 0.1$. The spin-2 nature of the graviton results in either s wave (diphoton) or p wave (dilepton) decay products, giving a branching fraction in a single dilepton channel half that in the diphoton channel [3]. This analysis searches for the first excited mode in the diphoton final state using 5.4 fb^{-1} of Run II data. This work develops from a previous diphoton search performed in 1.1 fb^{-1} of diphoton data [4].

2 Data and Monte Carlo samples

The datasets used in this analysis are cdip and cph1, all in the Stntuple format, covering the periods 0-25 of data taking. The good run list used is goodrun_v31_pho_00.txt [5] which corresponds to an integrated luminosity of 5.36 fb^{-1}. Signal samples for $G \to \gamma\gamma$ RS gravitons are generated using Pythia version 6.226.[1] Mass points (m_G) are taken at 100 GeV intervals from 200 GeV to 1100 GeV, with width $k/\overline{M}_{Pl} = 0.01$ (datasets **re0s(0-9,a-i)s**). There are about 300,000 diphotons events for each graviton mass. For the MC modeling of the QCD diphoton background, the Pythia diphoton dataset **gx0s1g** in Stntuple format is used.

3 Event selection and corrections

The diphoton triggers, base event selection, and photon identification requirements are exactly the same as the analysis documented in [4]. The data are required to have passed one of the following trigger paths: DIPHOTO_12, DIPHOTON_18, ULTRA_PHOTO_50 or SUPER_PHOTON_70 EM or JET. The SUPER_PHOTON_70 trigger only applies a loose E_T cut and a loose Had/EM cut, which prevents a potential inefficiency arising at high E_T where the EM energy becomes saturated causing the HAD/EM to be miscalculated. Since we only explore the diphoton mass spectrum above 100 GeV, the trigger efficiency is taken as 100%.

All events are first required to be marked "good" for photons using the goodrun lists. To select events consistent with a beam-beam interaction, the event must have a class 12 vertex and the primary z-vertex of the event has to be in the range $|Z_{event}| < 60$ cm. Events are then selected using the standard baseline analysis cuts for high p_T central photons. The χ^2 selection has been loosened from the standard $\chi^2 < 20$ to $\chi^2 < 50$ for $E_T > 50$ GeV to remove a strong E_T dependence in the χ^2 efficiency seen in the RS MC. All events are required to have two photons in the central region. In the case of events with more than two photons passing the identification cuts, the two photons with the highest transverse energies are selected. In addition, both photons are required to have a transverse energy (E_T) > 15 GeV and an invariant mass ($M_{\gamma\gamma}$) > 30 GeV. We only fit the diphoton mass spectrum in the region $M_{\gamma\gamma} > 100$ GeV.

Reference [6] uses $Z \to ee$ events in data and MC to derive a energy scale correction,

[1] This is newer than the version 6.216 in the standard setup. In the version 6.223, Pythia introduced a fix to the line shape of the RS graviton decays to be consistent with the spin 2 nature of the graviton.

based on comparing the MC and data Z mass peaks. This energy scale correction is applied to this analysis.

Reference [7] uses $Z \rightarrow ee$ events in data and MC to derive a correction to the photon ID cut efficiency reported by the MC. Following the same procedure described in [6], we weight the correction by the period luminosities, and the observed NVertex distributions to find an overall multiplicative efficiency correction of 0.967 per photon. In addition, there is some indication of an E_T-dependence, so we let the 0.967 go linearly to 1.0 between 40 and 80 GeV, and then pin it to 1.0 above 80 GeV.

4 Signal efficiency

4.1 Efficiency

Figure 1 shows the reconstructed diphoton mass of $G \rightarrow \gamma\gamma$ events that pass the event selection. The width of the distribution is primarily determined by the detector resolution. The graviton decay width depends on the graviton mass and $k/\overline{M}_{Pl}$. For the n^{th} KK excitation, the graviton width is

$$\Gamma_n = \rho m_n x_n^2 (k/\overline{M}_{Pl})^2, \tag{3}$$

where ρ is a constant depending on the number of open decay channels. At $m_G = 1.1$ TeV, the decay width is $\Gamma_1 = 0.15$ GeV for $k/\overline{M}_{Pl} = 0.01$. This is negligible compared to the detector resolution. The distributions become clearly asymmetric at high masses. This is most likely caused by the leakage in the calorimeter rather than the saturation of readout. For the maximal graviton mass $m_G = 1.1$ TeV, a single photon is expected to deposit 550 GeV energy in the calorimeter tower on average. The system is designed to saturate by the ADC counts rather than the PMTs. The saturation occurs at around 700 GeV which is higher than the average energy we expect in the calorimeter tower for 1.1 TeV RS gravitons.

Figure 2 shows the efficiency of selecting $G \rightarrow \gamma\gamma$ events as a function of the graviton mass. The error bars represent the systematic errors, which will be discussed in the next section. The efficiency shows a strong dependence on the graviton mass. This is driven by the detector acceptance. The low mass graviton decays are more likely to produce photons in the plug calorimeter. Table 1 shows the total efficiency and systematic error for RS graviton events decaying to two photons as a function of graviton mass.

4.2 Systematic uncertainties

This section summarizes the systematic uncertainties we evaluated on the signal selection efficiency.

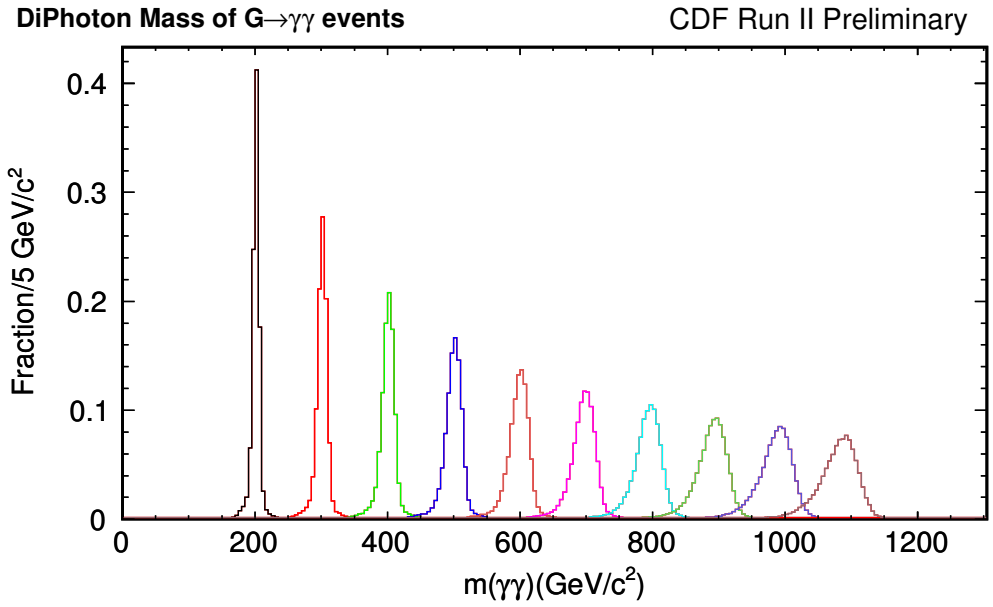

Figure 1: Reconstructed diphoton mass of $G \to \gamma\gamma$ events that pass the event selection. Samples of various graviton masses are shown in different colors.

Graviton Mass (GeV)	Total Efficiency and Systematic Error
200	0.118 ± 0.014
300	0.175 ± 0.021
400	0.224 ± 0.026
500	0.258 ± 0.029
600	0.284 ± 0.030
700	0.299 ± 0.029
800	0.312 ± 0.027
900	0.321 ± 0.029
1000	0.330 ± 0.027
1100	0.334 ± 0.026

Table 1: Total efficiency and systematic error for RS graviton events decaying to two photons as a function of graviton mass.

4.2.1 PDF

The PDF uncertainty on signal efficiency is calculated using the CTEQ6M [8] error sets. We employ an event re-weighting technique to calculate the efficiency using different PDFs and the fractional difference is taken as the systematic error.

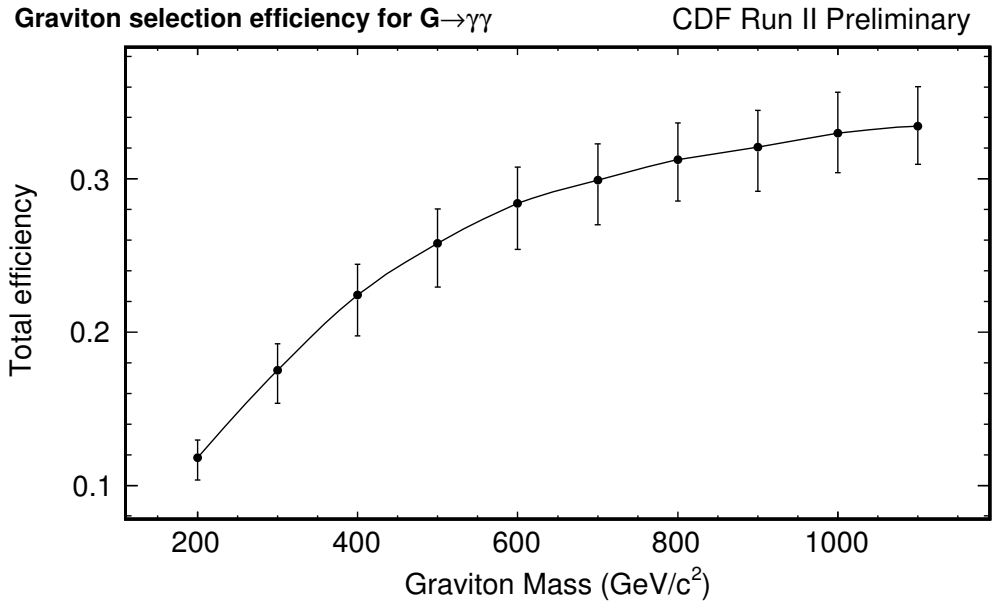

Figure 2: The efficiency of selecting $G \to \gamma\gamma$ events as a function of the graviton mass. The error bars represent the systematic errors.

4.2.2 ISR/FSR

The change in acceptance due to more or less initial and final state radiation (ISR/FSR) is calculated using Pythia, by varying the parton shower parameters as prescribed by the Joint Physics Group [9].

4.2.3 Q^2(Scale)

The scale uncertainty on acceptance is calculated by varying the Pythia scales used in the parton distributions and α_s.

4.2.4 Energy scale

Reference [4] studies the systematic effect on the acceptance due to an E_T scale offset by varying the 15 GeV threshold by ±1%, which is the uncertainty on the energy scale. The maximal fractional difference in acceptance is 0.1% for central-central diphotons. We take 0.1% as the systematic error associated with the energy scale uncertainty for this analysis.

4.2.5 Z vertex

Reference [4] studies the z vertex efficiency by comparing the fraction of events in which the interaction takes place within the ± 60 cm in data and in RS MC. This results in

a 0.2% systematic uncertainty on the efficiency which is used for this analysis.

4.2.6 $Z \to ee$ based efficiency correction

The Z-based efficiency correction has an uncertainty from several sources [7], including uncertainty in the material leading to lost conversion events and the difference between electrons and photons. This systematic error is taken as 3% conservatively.

4.2.7 Integrated luminosity

This systematic source accounts for the uncertainty in the $p\bar{p}$ inelastic cross section and for the uncertainty in the acceptance of the luminosity monitor of CDF to inelastic $p\bar{p}$ collision events and it is estimated as 6%. This uncertainty is applied to the rate prediction based on signal Monte Carlo simulation.

4.2.8 Total systematic uncertainty

Figure 3 shows the combination of the systematic uncertainties on the signal prediction as a function of the graviton mass.

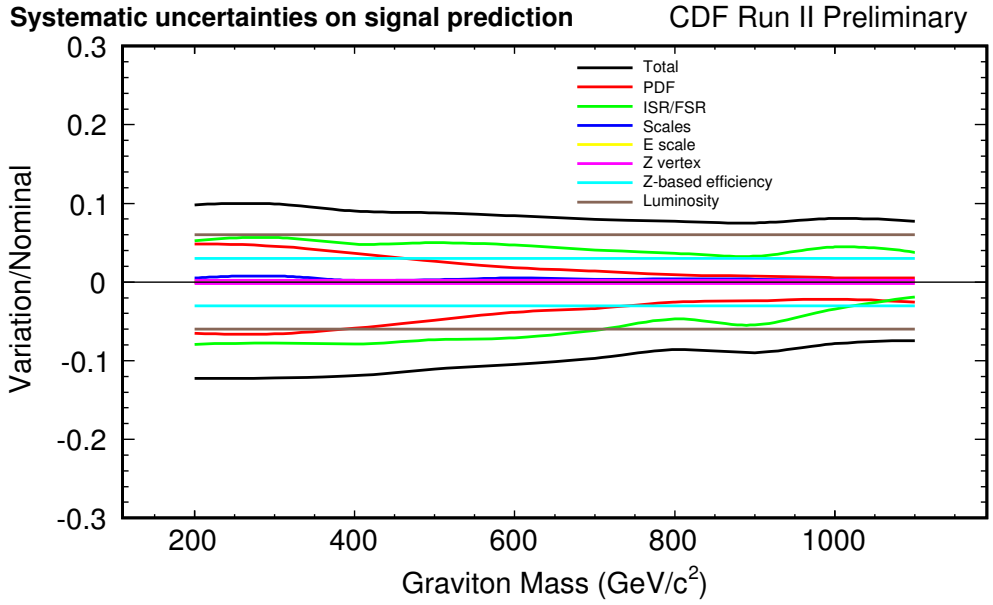

Figure 3: The systematic uncertainties on the signal prediction.

5 Background estimation

The two main sources of background in the $G \to \gamma\gamma$ search come from Standard Model diphoton production and from one or two jets faking photons.

5.1 Background from Standard Model diphoton production

5.1.1 DiPhox

The Standard Model diphoton background is calculated based on the DiPhox NLO cross section MC [10]. This program calculates the kinematics and cross sections of a $h_1 + h_2 \to 2\gamma + h_3$ process on an event-by-event basis, where the particles $h_{1,2,3}$ are hadrons. Each event may or may not have an unobserved hadron h_3 in the final state. We apply the kinematic cuts to ensure that the phase space is consistent with data. The cuts applied are on the transverse momentum $p_T^\gamma \geq 15$ GeV and rapidity $|y^\gamma| \leq 1$ of each photon. In addition to these, the isolation cut is also applied on both photons in each event by defining a cone of radius $R = \sqrt{(\Delta y)^2 + (\Delta\phi)^2}$ and axis along the direction of each photon and requiring that 1) $\Delta R > 0.4$ between two photons and 2) if the direction of the unobserved hadron lies within this cone (for events with 3-particle final state) then its transverse momentum is $p_T^{h_3} \leq 2$ GeV. The CTEQ6M PDF is used and the scales are chosen to be $\mu_F = \mu_f = \mu_R = M/2$, where M is the diphoton mass. We only take into account the contributions from direct and one fragmentation processes. The contribution from two fragmentation process is negligible (0.2%) [6]. Fragmentation contributions are highly suppressed by the isolation cut.

Figure 4 shows the DiPhox distribution fit to a general function form (5 exponentials):

$$y = (x^{0.1} + \alpha_0 x^{\alpha_1})(e^{x/\alpha_2} + \alpha_3 e^{x/\alpha_4} + \alpha_5 e^{x/\alpha_6} + \alpha_7 e^{x/\alpha_8} + \alpha_9 e^{x/\alpha_{10}}), \tag{4}$$

where x is the mass minus the mass threshold cut of 30 GeV and α's are fit parameters.

5.1.2 Diphoton selection efficiency

The DiPhox cross section is multiplied by the mass-dependent diphoton identification efficiency, which is measured using the Pythia diphoton MC **gx0s1g**, to give the prediction of Standard Model diphoton background. We fit a straight line to this efficiency as a function of mass for mass > 100 GeV as shown in Figure 5.

5.1.3 Systematic uncertainties

A lot of systematic uncertainties on Standard Model diphoton background are evaluated in the same way as for the signal efficiency. These systematic effects are integrated luminosity, PDF, ISR/FSR and $Z \to ee$ based efficiency correction. The following systematics are also included in the background prediction.

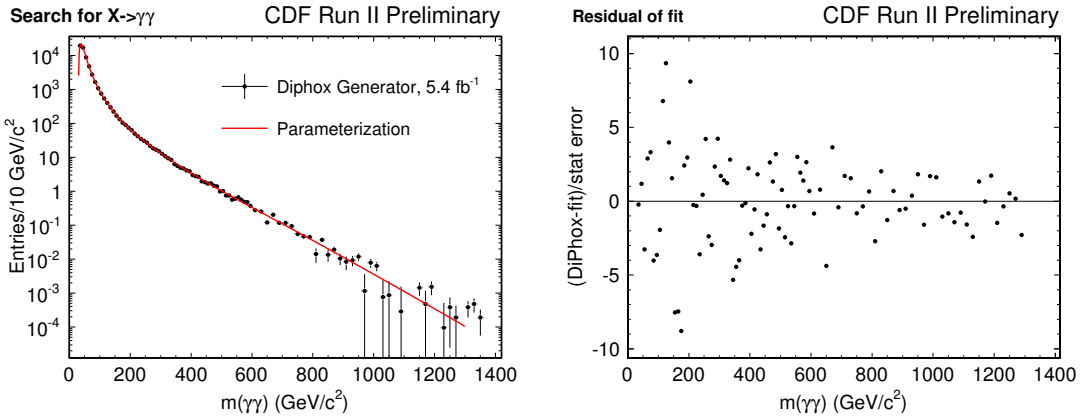

(a) DiPhox spectrum

(b) Residual of fit

Figure 4: The DiPhox cross section for Standard Model diphoton production.

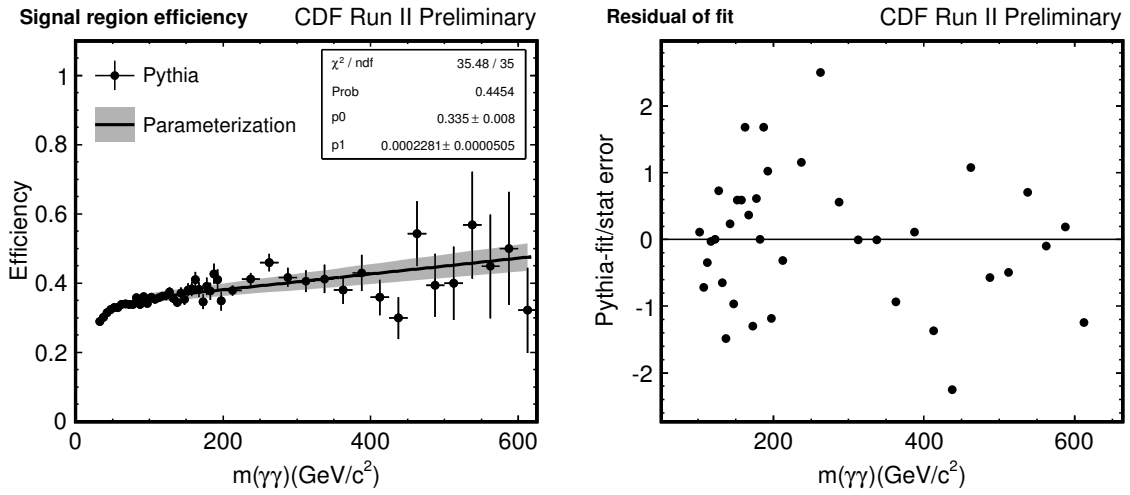

Figure 5: Reconstructed mass of all events passing the selection criteria, divided by the generated mass of all events passing the E_T, η and isolation cut at generator level, measured by Pythia. A linear fit is shown with its uncertainty.

The uncertainty associated with the fit to the diphoton selection efficiency is shown in Figure 5.

We evaluate the uncertainty on the diphoton cross section due to variations in the Q^2 scale by running DiPhox with two different scales settings: $\mu_F = \mu_f = \mu_R = M$ and $\mu_F = \mu_f = \mu_R = M/4$ and take the differences with respect to the default setting as the systematic error.

We take 6% (3% per photon) as the uncertainty due to underlying events [11].

Figure 6 shows the combination of the systematic uncertainties on the SM diphoton background prediction.

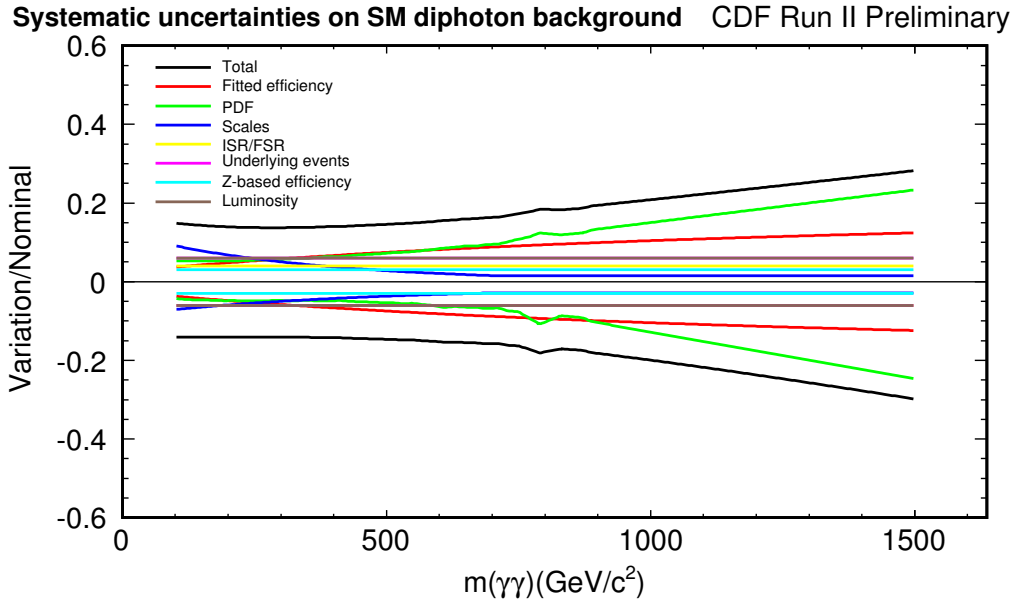

Figure 6: The systematic uncertainties on the SM diphoton background prediction.

5.2 Background from jets faking photons

Approximately 75% of diphoton data events contain one or two fake photons. These come from jets, primarily quark jets fragmenting to a hard leading π^0. This background is estimated by fitting the data diphoton mass spectrum with the DiPhox prediction plus a general function form, which will be discussed in the next section.

6 RS graviton cross section limits

6.1 Background fit

We fit the data central-central diphoton mass distribution to the DiPhox prediction plus a function form similar to Eq.(4) but with only 2 exponentials (setting $\alpha_{5-10} = 0$), which represents the contribution of jets faking photons. The 2 exponentials function form was justified to well describe the jets faking photons in the last analysis by fitting the sideband distributions [4]. The DiPhox prediction is fixed. We only fit data above 100 GeV since the lowest graviton mass we are exploring is 200 GeV. The fit is shown in Figure 7. The residual and integral are shown in Figure 8. If we allow the DiPhox prediction to float, we get very similar result and the best fit normalization of DiPhox

is 1.016. This indicates that the default DiPhox describes the data distribution very well at high masses.

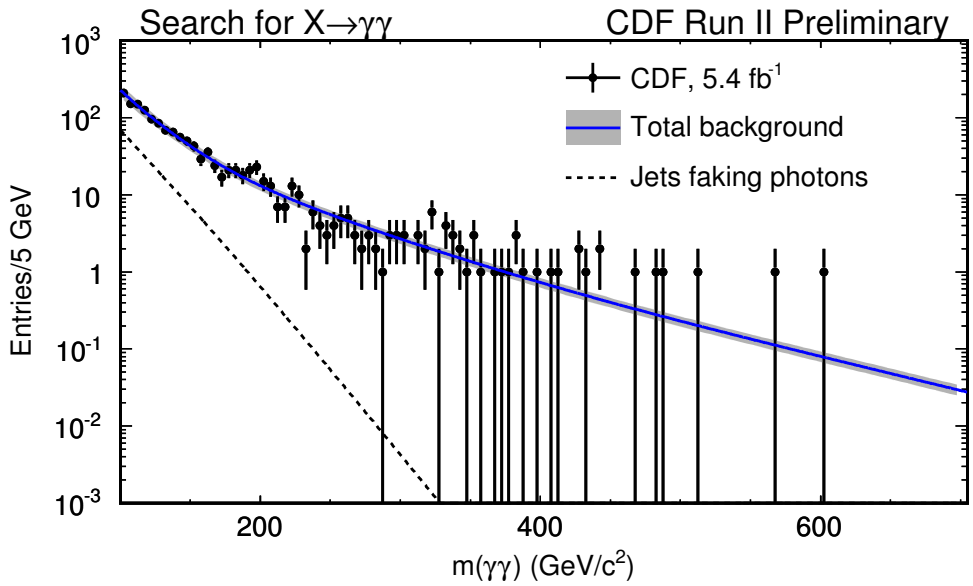

Figure 7: The distribution of data central-central diphoton events with the fit overlaid. The DiPhox prediction is fixed. The systematic uncertainty on DiPhox prediction is shown as gray error band.

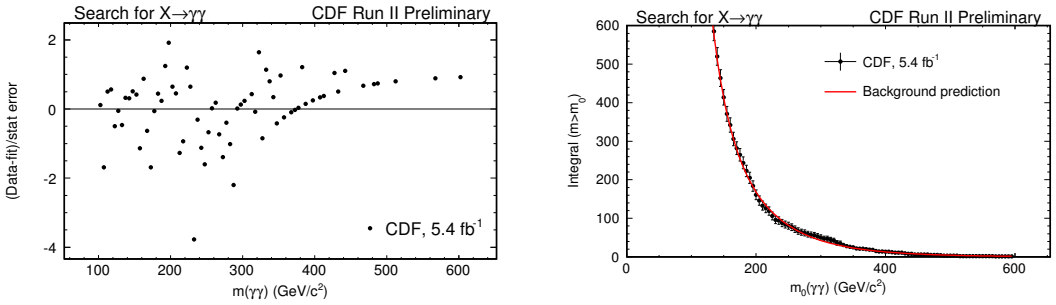

(a) Residual (b) Integral

Figure 8: The residual and integral of the fit.

6.2 Limits on RS model

To calculate the limits we use the CL_s method implemented by Tom Junk [12]. The confidence level for excluding H_1, given some experimental data and a null hypothesis

H_0, is based on the quantity

$$CL_s = \frac{P_{H_1}(\Delta\chi^2 \geq \Delta\chi^2_{obs})}{P_{H_0}(\Delta\chi^2 \geq \Delta\chi^2_{obs})}. \quad (5)$$

The probabilities in the denominator and numerator are calculated by generating pseudo-experiments using the signal and background templates. The 95% CL limit on the RS cross section corresponds to $CL_S = 0.05$. The signal and background templates are described in the previous sections. We assign a conservative systematic error of 50% to the jets faking photon background but this should not affect the limits in the region we are interested in.

Figure 9 shows the observed limit together with the expected limits from pseudo-experiments. The observed limit is more than 2 σ away from the expected limit at 200 GeV. We look closely at data distribution around 200 GeV and we indeed see a small bump there (Figure 10).

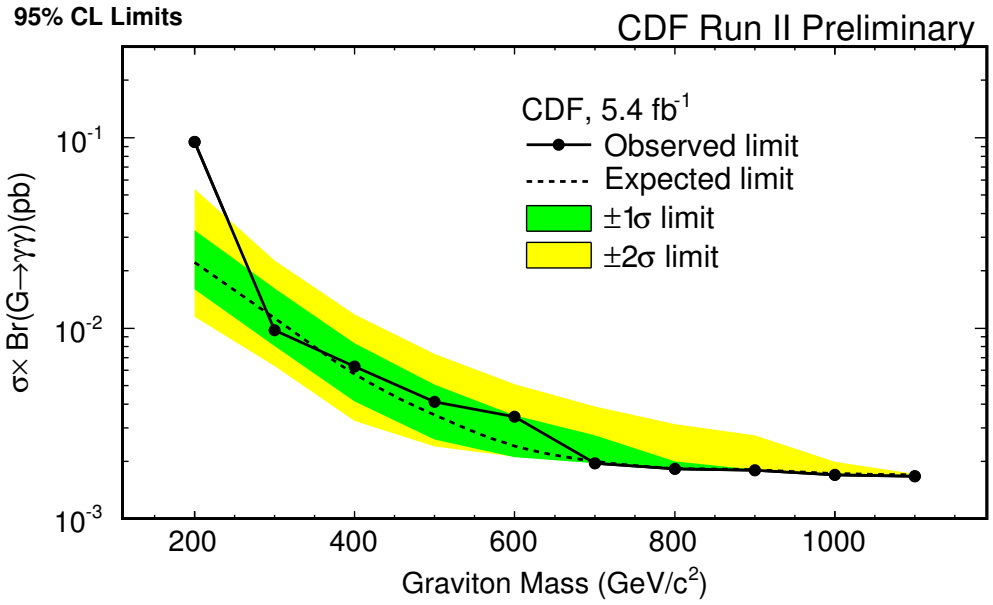

Figure 9: 95% CL limit for data with the expected limits from pseudo-experiments.

To understand the significance of the excess at 200 GeV, a frequentist model independent search for an excess over SM predictions on diphoton events in an invariant mass range of 150 - 650 GeV is performed, following the procedure outlined in [13]. The probability for the background to fluctuate to the level observed in the data or higher, referred to as the p-value, is calculated using Poisson statistics in a mass window comparable to the detector resolution. The uncertainty on the background estimate is treated as a nuisance parameter and it is integrated out assuming it is Gaussian distributed. The result is shown in Figure 11. The lowest p-value observed is at

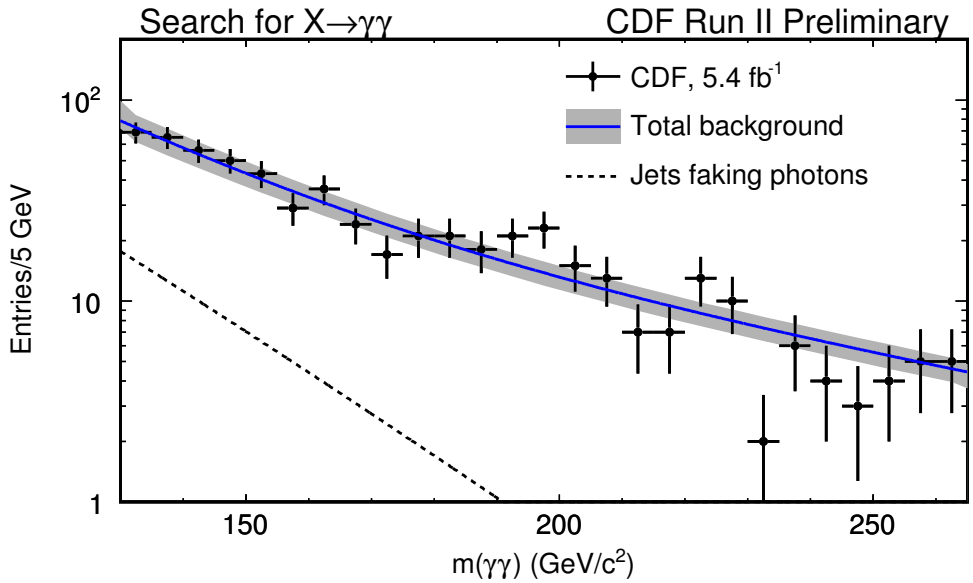

Figure 10: A bump around 200 GeV.

$m(\gamma\gamma) \approx 198$ GeV, for which the background has a probability of 0.013 of fluctuating to the level of data or higher. However, due to the large search range, there are many individual measurements which mean that it is increasing likely to find large upward deviations from the background in the data by chance. To take this into account, the method is repeated for 200,000 pseudo-experiments produced using only the predicted background distribution as a template. This gives an expected range for the minimum p-value in the mass spectrum to lie, together with the p-value necessary to claim 3 σ evidence of new physics, both of which are shown in Figure 11. As the lowest observed p-value is within the expected range, it indicates that the excess at $m(\gamma\gamma) \approx 198$ GeV is consistent with a statistical fluctuation and therefore it is concluded that the results of this analysis are consistent with the SM.

Table 2 shows the number of background events and the number of signal events at 95% CL cross section limit. The number of background events is integrated between $\pm 2\sigma_D$ where σ_D is the detector resolution.

The 95% CL upper limit on $\sigma \times BR(G \to \gamma\gamma)$ as a function of graviton mass is shown in Figure 12, with the theoretical cross sections for widths 0.01, 0.025, 0.05, 0.07 and 0.1, which are obtained by scaling the $k/\overline{M}_{Pl} = 0.1$ cross sections. The leading-order graviton production cross section is multiplied by a K factor to correct for diagrams at higher-order in α_s. Figure 13 shows the K factor for $G \to \gamma\gamma$ as a function of graviton mass [14]. The dependence of K factor on $k/\overline{M}_{Pl}$ is negligible.

The 95% CL lower limits on the mass of the RS graviton are determined by the position of the intersection of the theoretical cross sections and the limit on the cross section times branching ratio. The 95% CL excluded region in the $k/\overline{M}_{Pl}$ and graviton

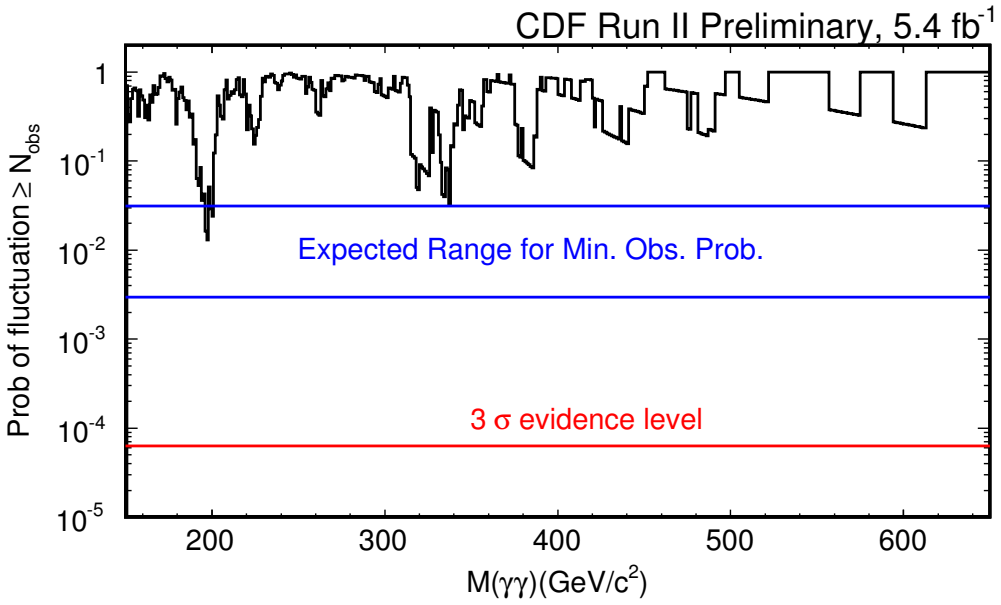

Figure 11: The probability of the background to fluctuate to the level of the data or higher in a mass window comparable to the detector resolution. The expected range is the range in which the minimum p-values of 68.3% of pseudo-experiments lie with the tails being symmetric. The 3 σ evidence line corresponds to the p-value above which 99.7% of the pseudo-experiments fall.

Mass (GeV)	Number of background events	Number of signal events at 95% CL limit
200	46	59
300	13	8.8
400	4.8	7.4
500	1.9	5.6
600	0.79	5.2
700	0.33	3.1
800	0.13	3.0
900	0.052	3.0
1000	0.019	3.0
1100	0.0072	3.0

Table 2: The number of background events and the number of signal events at 95% CL cross section limit.

mass plane is shown in Figure 14. Also shown is the excluded region of the previous analysis with an integrated luminosity of 1.1 fb^{-1}. The updated analysis improves the limits significantly. Table 3 shows the mass limits for varying values of $k/\overline{M}_{Pl}$.

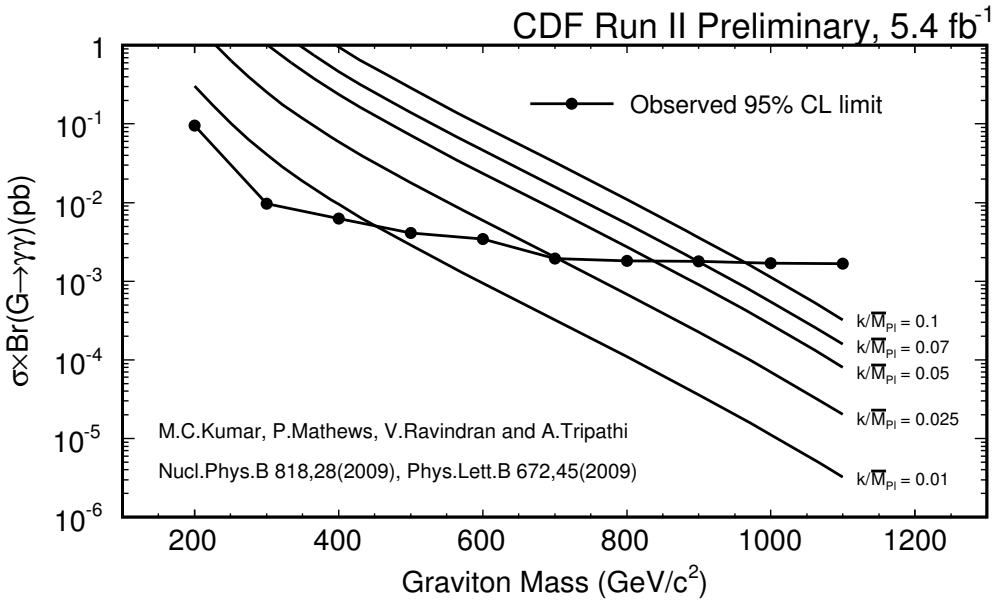

Figure 12: 95% CL upper limit on the production cross section times branching fraction of an RS model graviton decaying to diphotons as a function of graviton mass. Also shown are the predicted $\sigma \times BR$ curves for $k/\overline{M}_{Pl} = 0.01$, 0.025, 0.05, 0.07 and 0.1.

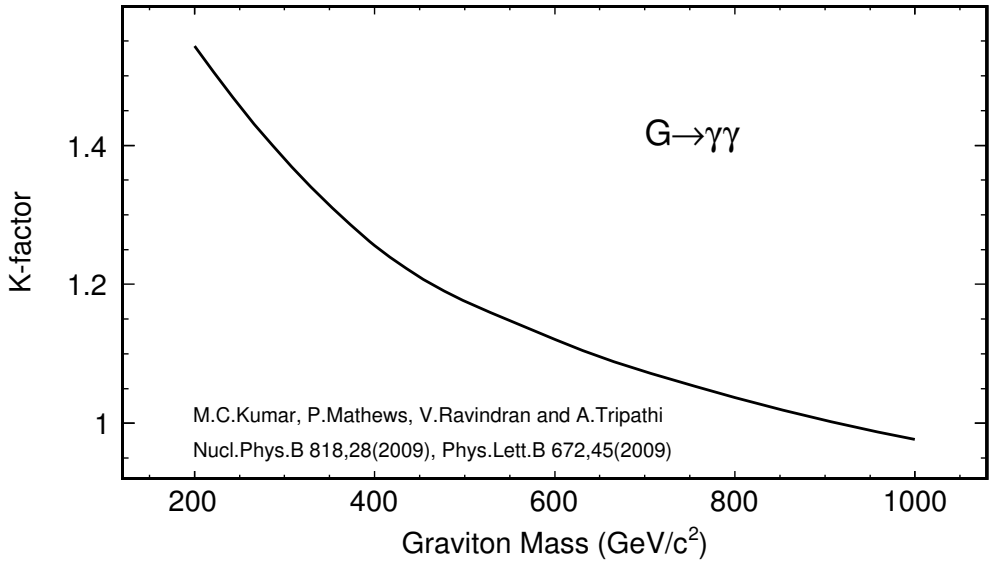

Figure 13: NLO K-factor for $G \to \gamma\gamma$ as a function of graviton mass [14].

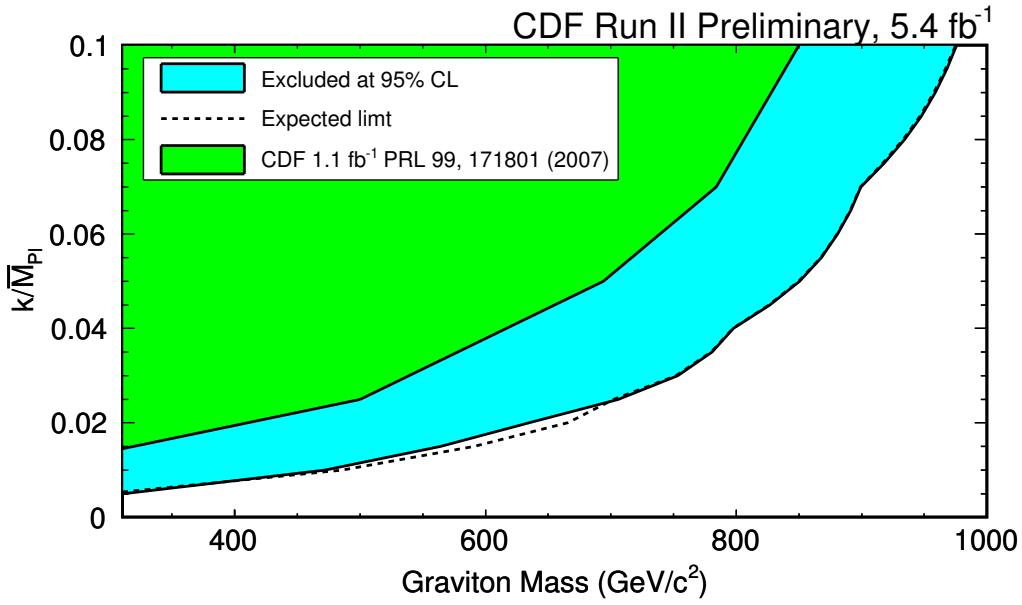

Figure 14: 95% CL excluded region on the plane for graviton mass vs $k/\overline{M}_{Pl}$.

$k/\overline{M}_{Pl}$	Lower Mass Limit (GeV) 5.4 fb^{-1}	Lower Mass Limit (GeV) 1.1 fb^{-1} [4]
0.1	976	850
0.07	899	784
0.05	850	694
0.025	706	500
0.01	472	230

Table 3: The 95% CL lower limits on the RS graviton mass for varying values of $k/\overline{M}_{Pl}$.

7 Summary

A search for a Randall-Sundrum graviton in the diphoton decay mode has been performed in the central-central channel, using an integrated luminosity of 5.4 fb^{-1} of Run II data. The observed diphoton invariant mass spectrum is consistent with the expected background. A 95% confidence level limit on the production cross section times branching ratio for a graviton decaying to diphotons as a function of the diphoton invariant mass is obtained. In addition 95% confidence level lower limits on the masses of the Randall-Sundrum graviton are determined.

A Comparison with D0

Figure 15 shows the comparison with D0 limits. D0 has better limits for two reasons. First ,they use a constant K factor of 1.54. Secondly, they search for RS gravitons in both diphoton and dielectron channels. We recalculated the limits with a constant K factor of 1.54 and the resulting limits are shown as the red curve. The remaining difference is due to the inclusion of dielectron events in the D0 analysis.

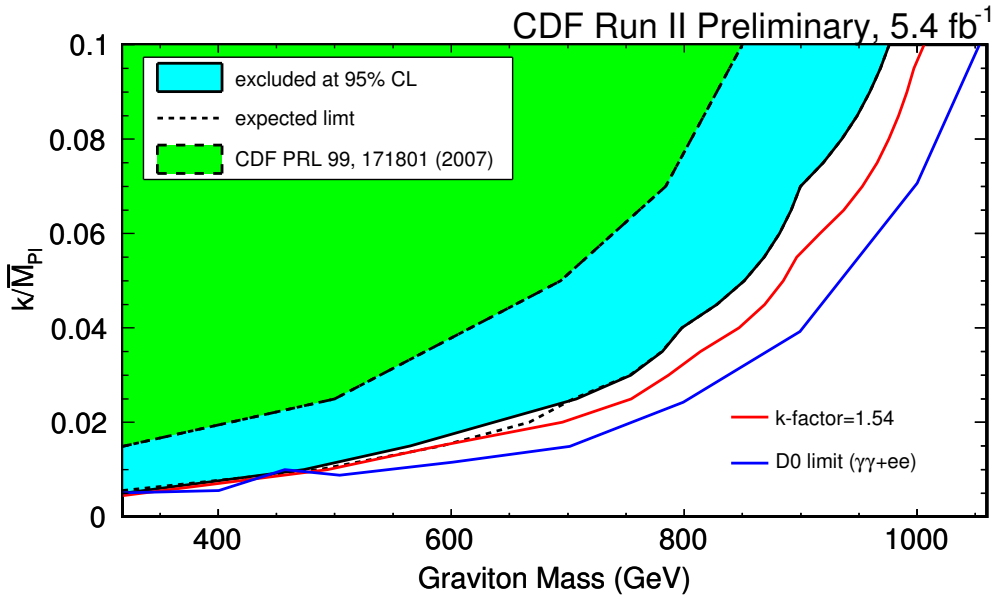

Figure 15: 95% CL excluded region on the plane for graviton mass vs $k/\overline{M}_{Pl}$. CDF limits with $K = 1.54$ and D0 limits are also shown.

References

[1] N. Arkani-Hamed, S. Dimopoulos and G. R. Dvali, Phys. Lett. B **429**, 263 (1998) [arXiv:hep-ph/9803315]; Phys. Rev. D **59**, 086004 (1999) [arXiv:hep-ph/9807344]; I. Antoniadis, N. Arkani-Hamed, S. Dimopoulos and G. R. Dvali, Phys. Lett. B **436**, 257 (1998) [arXiv:hep-ph/9804398].

[2] L. Randall and R. Sundrum, Phys. Rev. Lett. **83**, 3370 (1999) [arXiv:hep-ph/9905221].

[3] H. Davoudiasl, J. L. Hewett and T. G. Rizzo, Phys. Rev. Lett. **84**, 2080 (2000) [arXiv:hep-ph/9909255].

[4] S-M Wynne *et al*, "Search for Randall-Sundrum Gravitons in 1155 pb^{-1} Run II High Mass Diphoton Data", CDFNote 8359, January 2007.

[5] http://www-cdf.fnal.gov/internal/physics/photon/goodrun.html

[6] Ray Culbertson *et al*, "Measurement of the central diphoton production cross section at CDF", CDFNote 10009, November 2009.

[7] Craig Group *et al*, "Photon Efficiency Scale Factors (up to p12)", CDFNote 9429, November 2008. The same efficiency correction was studied to p23 by Karen Bland, https://hep.baylor.edu/hep/kbland/374 We assume the corrections for P24-25 are ths same as P18-23.

[8] J. Pumplin *et al*, JHEP 0207:012(2002), hep-ph/0201195

[9] CDF Joint Physics Group
http://www-cdf.fnal.gov/internal/physics/joint_physics/

[10] T. Binoth, J. P. Guillet, E. Pilon and M. Werlen, Eur. Phys. J. C **16**, 311 (2000) [arXiv:hep-ph/9911340].

[11] Ray Culbertson *et al*, "Measurement of the inclusive and isolated prompt photon cross section at CDF", CDFNote 9590, April 2009.

[12] Tom Junk *et al*, "Sensitivity, Exclusion and Discovery with Small Signals, Large Backgrounds, and Large Systematic Uncertainties", CDFNote 8128, October 2007.

[13] S Harper, "The Search for New Physics in High Mass Di_Electron Events in $p\bar{p}$ Collisions at $\sqrt{s} = 1.96$ TeV", CDFNote 8694, February 2007.

[14] M. C. Kumar, P. Mathews, V. Ravindran and A. Tripathi, Nucl. Phys. B **818**, 28 (2009) [arXiv:0902.4894 [hep-ph]]; M. C. Kumar, P. Mathews, V. Ravindran and A. Tripathi, Phys. Lett. B **672**, 45 (2009) [arXiv:0811.1670 [hep-ph]]; private communications with the authors.